NANO LETTERS

2008
Vol. 8, No. 7
2070-2076

Enhanced Cellular Activation with Single Walled Carbon Nanotube Bundles Presenting Antibody Stimuli

Tarek R. Fadel,‡ Erin R. Steenblock,† Eric Stern,† Nan Li,‡ Xiaoming Wang,‡ Gary L. Haller,‡ Lisa D. Pfefferle,‡ and Tarek M. Fahmy*,†,‡

Department of Biomedical Engineering, and Department of Chemical Engineering, Yale University, P.O. Box 208284, New Haven, Connecticut 06520

Received February 3, 2008; Revised Manuscript Received April 16, 2008

ABSTRACT

Efficient immunotherapy can be accomplished by expanding T cells outside the body using single walled carbon nanotube (SWNT) bundles presenting antibody stimuli. Owing to the large surface area of these bundles, which can reach 1560 m^2/g, T cell stimulating antibodies such as anti-CD3, can be presented at high local concentrations inducing potent activation of T cells. We show that anti-CD3 adsorbed onto SWNT bundles stimulate cells more effectively than equivalent concentrations of soluble anti-CD3. Stimulation by antibody adsorbed onto SWNT is significantly higher than other high surface area materials (activated carbon, polystyrene, and C60 nanoparticles), suggesting unique properties of SWNT bundles for stimuli presentation. We demonstrate the surface area tunability of these bundles by chemical treatment and its effect on antibody adsorption and subsequent T cell activation. In addition, the T cell response varied with the concentration of SWNT in a concentration dependent manner. Antibody stimuli adsorbed onto SWNT bundles represent a novel paradigm for efficient activation of lymphocytes, useful for basic science applications and clinical immunotherapy.

Single walled carbon nanotubes (SWNT) are an emerging biomaterial with applications ranging from electronics,[1] drug delivery,[2,3] imaging,[4] and biosensing.[5] Due to their unique physio-chemical properties, SWNT can be adapted to a wide range of applications in the field of nanotechnology and bioengineering. Recent investigations have focused on new methods of biochemical functionalization of carbon nanotubes using various proteins for potential applications in biological systems.[3,6–10] Proteins can be attached covalently through reaction with the functionalized SWNT surface,[8,11] or noncovalently by nonspecific adsorption.[3,12] In this study, we focus on the latter method, as we explore the use of SWNT bundles in presenting T cell activating antibodies.

T cells are central players in initiating and maintaining immune responses. An important goal of successful immunotherapy is the stimulation of T cell immune responses against targets of interest such as tumors.[13,14] This can be accomplished in two ways:[15] (1) through immunization with tumor antigens or (2) by isolation of T cells specific to tumor antigen, and expansion of this population outside the body followed by retransfer into the patient (adoptive cell transfer therapy).[16,17] Some of the most encouraging data regarding immunotherapy come from studies employing adoptive transfer of tumor reactive T cells.[18–20]

Specific expansion of T cells outside the body depends however on efficient methods for displaying protein−ligands that stimulate those cells. The display of T cell stimuli on artificial substrates is referred to as artificial antigen-presentation.[21–23] This represents a new effort to generate a reproducible "off-the-shelf" means of stimulating and expanding T cells in vitro. Several types of artificial antigen-presenting cells (aAPCs) have been developed, including nonspecific bead-based systems that are currently used in many research laboratories to sustain the long term expansion of $CD8^+$ T cells.[22,23]

Ultimately, T cell stimulus intensity depends on the density of bound receptors in contact with a surface.[24,25] Regions with a high density of T cell antigen receptors have been termed activated clusters because they are critical for T cell stimulation.[26,27] The presence of such high density clusters has also been shown to accelerate T cell activation.[25] In the lymph node, the primary site for T cell stimulation, antigen presenting cells are thought to concentrate the presentation of T cell stimuli by trafficking in a dense architectural scaffolding in close proximity to T cells.[28] Because of the significance of this density requirement, particle systems such as magnetic beads, polystyrene beads, liposomes and exosomes, and flat substrates such as polystyrene plates have been utilized as substrates for immobilizing T cell antigens for activation.[23] However, none of these systems offer the high surface area-to-volume ratio of SWNT. Thus, we

* Corresponding author. E-mail: Tarek.Fahmy@Yale.edu.
† Department of Biomedical Engineering.
‡ Department of Chemical Engineering.

10.1021/nl080332i CCC: $40.75 © 2008 American Chemical Society
Published on Web 06/12/2008

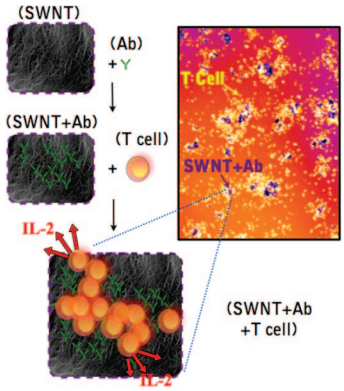

Figure 1. Schematic of anti-CD3-adsorbed SWNT scaffolds inducing T cell stimulation (not to scale). The SWNT scaffold is labeled as (SWNT), anti-CD3 as (Ab). The first step is adsorption of anti-CD3 by SWNT scaffold. After washing, the anti-CD3-adsorbed SWNT (SWNT + Ab) is incubated with T cells. Finally, the amount of T cell stimulation due to exposure to anti-CD3 in the activation platform (SWNT + Ab + T cell) is evaluated by measuring release of IL-2.

hypothesized that SWNT would function as powerful artificial antigen-presenting constructs for stimulation and expansion of T cells.

Here, we demonstrate that the T cell antigens (anti-CD3 antibodies, which is a known stimulus for T cell proliferation) can induce effective T cell stimulation when adsorbed onto SWNT. We show that antibodies against the T cell CD3 complex, when immobilized on SWNT, can activate T cells at concentrations at least an order of magnitude less than antibody alone. Furthermore, we demonstrate that this enhanced presentation efficiency is unique to SWNT bundles by showing that other high surface area materials, activated carbon, polystyrene nanoparticles, and buckyballs (C60), do not achieve similar activation levels. Thus, we illustrate the importance of density as well as qualitative geometry of the antigen-presenting substrate.

SWNT bundles for T cell stimulation are attractive for several reasons. First, the surface area for antibody adsorption can be tuned by altering the surface chemistry of the individual SWNT. Accessible surfaces that are a priori not available for protein adsorption can be made accessible through chemical treatment. Recent studies have demonstrated that acid treatment of SWNT induces defects on the surface of the nanotubes[29] as well as promotes debundling,[30] which can be correlated with an increase in surface area.[31] Second, the capacity of SWNT to irreversibly[12] adsorb protein antigens can be exploited to transform bundles of SWNT into a protein stimulus-presenting platform for specific stimulation of T cells. In the scheme shown in Figure 1, SWNT (chemically treated or untreated) are exposed to an antibody stimulus (anti-CD3). T cell activation was quantified via secretion of Interleukin-2 (IL-2), a critical cytokine secreted by T cells in response to an activating stimulus.[32] The schematic depicted in Figure 1 exploits the use of SWNT to improve standard methods of T cell activation, which typically involve immobilizing the same antibody on tissue culture polystyrene plate or use of the soluble antibody alone in solution.[32,33]

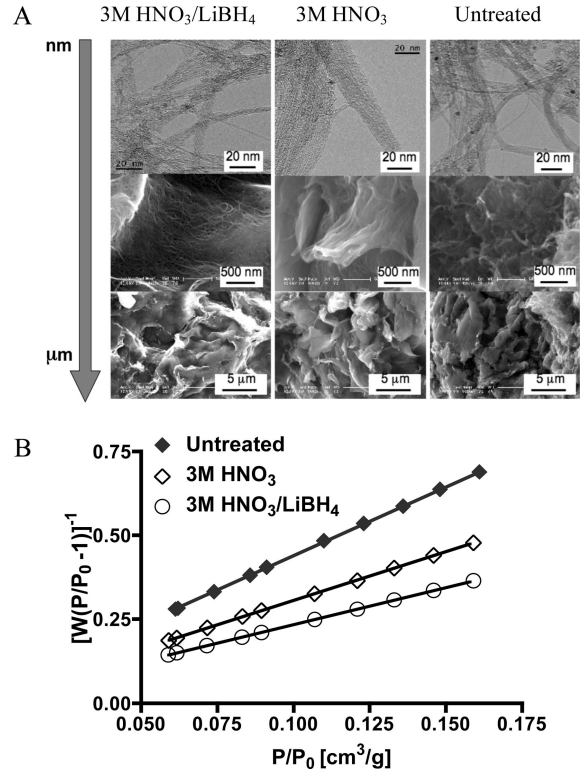

Figure 2. Physical characterization of treated and untreated SWNT bundles. (A) Electron microscope images presented in order of increasing biological length scales. Transmission electron micrography (first row) and scanning electron micrography (middle and last rows). TEM scale is 20 nm, SEM is 500 nm and 5 μm respectively (top to bottom). (B) BET plot of each SWNT group derived from nitrogen physisorption.

Table 1. B.E.T. Surface Area for SWNT Deduced from Nitrogen Physisorption

SWNT group	area (m^2/g)
untreated	845
3 M HNO_3	1190
3 M HNO_3/$LiBH_4$	1560

Our first goal was to examine the tunability of protein adsorption on SWNT through chemical treatment, which may affect the surface area for available protein interaction. We compared protein adsorption isotherms from untreated SWNT, SWNT treated with a 3 M nitric acid (3 M HNO_3), and SWNT treated with 3 M nitric acid then reduced in lithium borohydride (3 M HNO_3/$LiBH_4$) (see Supporting Information). We chose these treatments because refluxing SWNT in nitric acid introduces carboxylic acid groups at the open ends leading to sites of defects and hence enhancing capacity for protein adsorption.[29] A second step involving the reduction of the carboxylic groups in lithium borohydride will preferentially reduce the oxygenated groups created by previous acid treatment favoring the dispersion of SWNT in solution[34] and further increasing surface area available for protein adsorption.

We examined untreated and chemically treated SWNT at high magnification under transmission electron microscopy (TEM). We noted aggregated nanotube structures consistent with the bundling morphology (Figure 2A, top row). The

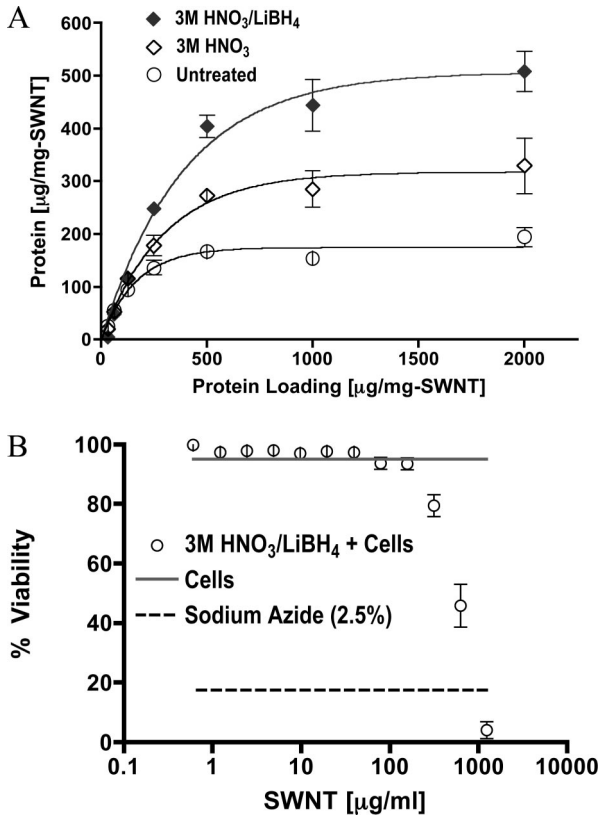

Figure 3. Biophysical characterization of treated and untreated SWNT bundles. (A) Adsorption isotherm of a model protein, bovine serum albumin (BSA). Data was fit using a one phase exponential association model. (B) Viability assay for T cells incubated with (3 M HNO_3/$LiBH_4$) SWNT bundles and a toxic salt (2.5% sodium azide).

three groups of SWNT showed similar structural integrity although some differences can be noted. First, the surface of nitric acid treated SWNT appeared to be slightly damaged when compared with untreated SWNT and can be correlated with the observed increase in the bundle surface area as measured by physiosorption.[31,35] Second, the nitric acid treatment appeared to reduce the amount of impurities, such as remaining catalysts present along with the nanotubes,[29,31,35,36] as seen by the reduction of metallic particles in the TEM images from Figure 2A. This purification step may play an important role in rendering the SWNT cytocompatible. The described chemical treatments do not induce gross morphological changes to the SWNT bundles. All three groups appeared as porous curved surfaces under scanning electron microscopy (Figure 2A, bottom row), with crevices on the length scale of cells, which may facilitate cellular interactions.

To ascertain the effect of these treatments on the surface area of the bundles, we estimated surface area using nitrogen physisorption.[31,35,37] As expected, the surface areas derived from Figure 2B using Brunauer−Emmett−Teller (B.E.T.) analysis, and summarized in Table 1, changes with the associated chemical treatment. Untreated SWNT have the least surface area at 845 m^2/g. SWNT treatment with 3 M HNO_3 produced a surface area of 1190 m^2/g. Finally, SWNT treatment with 3 M HNO_3/$LiBH_4$ produced the largest increase in surface area at 1560 m^2/g. The reduction step

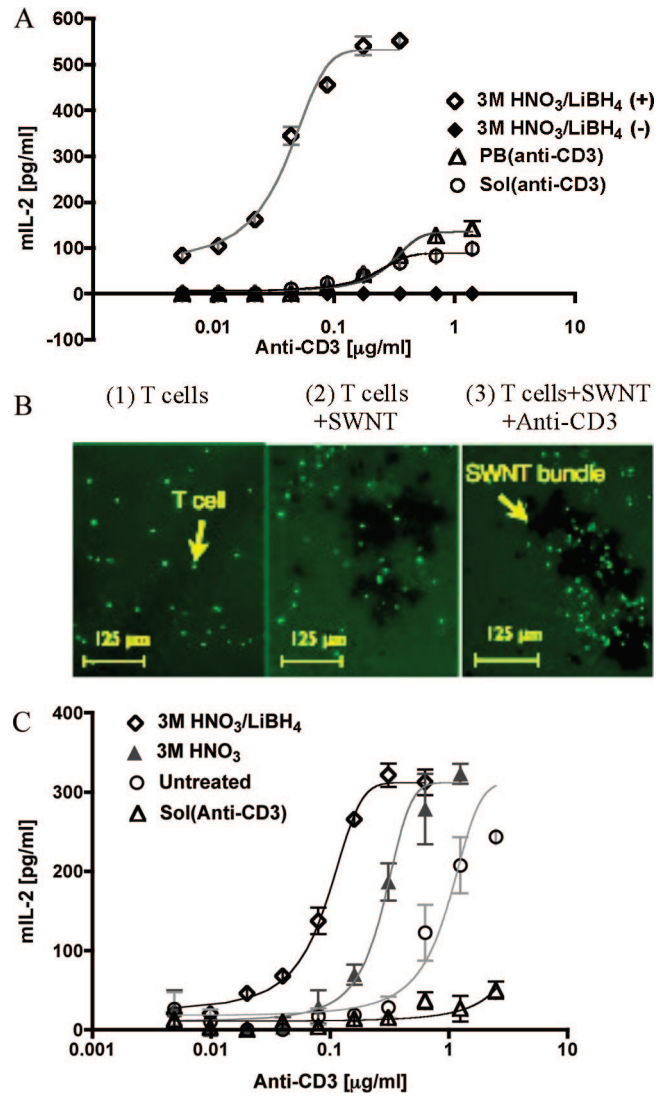

Figure 4. Enhanced stimulation of T cells by anti-CD3 adsorbed onto SWNT. (A) IL-2 release from T cells (B3Z) stimulated with anti-CD3-adsorbed (3 M HNO_3/$LiBH_4$) SWNT at 100 μg/ml labeled as 3 M HNO_3/$LiBH_4$ (+), plate bound anti-CD3 labeled as (PB) (anti-CD3), soluble anti-CD3 as Sol(anti-CD3) or blank 3 M HNO_3/$LiBH_4$ treated SWNT labeled as 3 M HNO_3/$LiBH_4$ (−). All groups except for 3 M HNO_3/$LiBH_4$ (−) were treated with the same concentration of anti-CD3. (B) Fluorescence microscopy of labeled T cells incubated with anti-CD3 adsorbed SWNT (3 M HNO_3/$LiBH_4$) or blank SWNT. Cells were stained with CFDA-SE staining solution. (T cells + SWNT) is an image of T cells incubated with blank SWNT bundle, (T cells + SWNT + anti-CD3) is an image of anti-CD3-adsorbed SWNT incubated with T cells and (T cells) is cells alone. Refer to Supporting Information for details on imaging protocol. (C) Stimulation of T cells by chemically treated SWNT adsorbed with antibody compared to soluble antibody. ELISA results for stimulation of B3Z cells as induced by anti-CD3 adsorbed onto (3 M HNO_3/$LiBH_4$) SWNT, anti-CD3 adsorbed onto (3 M HNO_3) SWNT, anti-CD3 adsorbed on (Untreated) SWNT and soluble anti-CD3 labeled as Sol(anti-CD3). All groups were treated with the same amount of anti-CD3. SWNT groups were introduced at a concentration of 50 μg/ml.

with $LiBH_4$ that follows the 3 M HNO_3 treatment may also play a role in enhancing SWNT surface area further through debundling,[30,31] although such a mechanism is not completely understood.

Table 2. Model Fit Parameters to a Concentration-Response Parametric Model[a]

		log [EC50]	R-squared
Figure 4 (A)	3 M $HNO_3/LiBH_4$ (+)	0.036 ± 0.002	0.977
	PB (Anti-CD3)	0.295 ± 0.020	0.952
	Sol (Anti-CD3)	0.213 ± 0.201	0.937
Figure 4 (C)	3 M $HNO_3/LiBH_4$	0.090 ±0.002	0.981
	3 M HNO_3	0.278 ±0.019	0.929
	Untreated	0.973 ± 0.081	0.830
	Sol (Anti-CD3)	N/A	N/A
Figure 5 (A)	100 μg/ml (+)	0.039 ± 0.002	0.975
	50 μg/ml (+)	0.080 ± 0.004	0.971
	25 μg/ml (+)	0.128 ± 0.005	0.979
	12.5 μg/ml (+)	0.250 ± 0.015	0.951
Figure 5 (B)	SWNT (3 M $HNO_3/LiBH_4$)	0.088 ± 0.004	0.980
	A.C. (Untreated)	2.286 ± 0.165	0.735
	A.C. (3 M HNO_3)	1.945 ± 0.104	0.876
	A.C. (3 M $HNO_3/LiBH_4$)	N/A	N/A
Figure 5 (C)	SWNT (3 M $HNO_3/LiBH_4$)	5.904−4 ± 0.001	0.980
	SWNT (3 M HNO_3)	2.242E-3 ± 0.001	0.931
	SWNT (Untreated)	7.285E-3 ± 0.001	0.913
	A.C. (Untreated)	5.830E-03 ± 0.001	0.816
	A.C. (3 M HNO_3)	0.0178 ±0.001	0.939
	PS-OH	2.091 ± 15.980	0.889
	PS-COOH	0.291 ± 0.061	0.906
	C60	N/A	N/A
	C60-OH	N/A	N/A

[a] PB (anti-CD3) refers to plate bound anti-CD3 and Sol (anti-CD3) refers to soluble anti-CD3. Refer to Supporting Information for more information on selected model.

To assess the effects of chemical treatment of SWNT bundles on protein adsorption, we incubated treated and untreated SWNT with a model protein, bovine serum albumin (BSA),[38] and measured the respective adsorption isotherms. Results are shown in Figure 3A. The adsorption curves show a correlation between the type of chemical treatment and the maximal protein adsorption. SWNT treated with 3 M $HNO_3/LiBH_4$ produced the highest measured surface area and subsequent higher protein adsorption. Thus, this treatment was selected for further studies on T cell stimulation. When scaled by molecular weight, the quantity of protein adsorbed is directly proportional to that offered in solution (see Supporting Information, Figure 2A). Thus, antibodies adsorb in the same manner as BSA but the total amount adsorbed is lower because of the 2.2-fold greater antibody size (150 kD versus 67 kD). From the data in Supporting Information, Figure 2A, we estimate that the amount of anti-CD3 adsorbed onto 3 M $HNO_3/LiBH_4$ /SWNT is 271 ± 45 μg per mg SWNT, compared with 508 ± 24 μg of BSA per mg SWNT, in good agreement with the theoretical factor.

Next, we assessed the cytocompatibility of SWNT modified with 3 M $HNO_3/LiBH_4$ on T cells. SWNT from this treatment group were titrated and incubated with T cells for 24 h before comparison to a cytotoxic control, sodium azide. We observed that treated SWNT did not present any significant toxic effects on T cells below a concentration of 150 μg/ml (Figure 3B). This minimal toxic effect observed with the treated nanotubes is expected since the overall length scale of SWNT bundles for cellular interaction is significantly larger than other reports which support SWNT toxicity.[39,40] In these reports, single tubes (significantly smaller than bundles) may be internalized causing the observed toxic effects. Thus, internalization of SWNT by T cells is improbable as the length of bundles is on the order of hundreds of nanometers to microns. A second possible reason for the observed minimal toxicity is the fact that chemical treatment of SWNT dissolves the majority of remaining impurities and metal catalysts from previous reactions.[29,31,35,36] This step could provide an improved environment for the proliferation of cells.[40,41] Also, the time scale needed for appropriate activation of T cells (see Supporting Information) is significantly shorter than most time scales involved in reported toxicity results.[40] Finally, the relatively high solubility of 3 M $HNO_3/LiBH_4$ SWNT in water could play a role in enhancing cytocompatibility.[42]

Table 3. B.E.T. Surface Area for Activated Carbon Deduced from Nitrogen Physisorption

A.C. group	area (m^2/g)
untreated	1762
3 M HNO_3	573
3 M $HNO_3/LiBH_4$	N/A

We investigated the stimulation of T cells using anti-CD3 adsorbed onto 3 M HNO_3 /$LiBH_4$ SWNT and compared this stimulation to anti-CD3 immobilized on tissue culture plate or free in solution. SWNT bundles incorporating the anti-CD3 stimulus had a dramatic effect on T cell activation as measured by the release of IL-2 (Figure 4A). Activation with antibody immobilized on SWNT was at least fourfold and sixfold greater in comparison to plate-bound antibodies and soluble antibodies, respectively. This was consistent with a model concentration−response fit[43] which suggested that the concentration of antibody at which half-maximal T cell stimulation takes place was significantly lower for antibody-SWNT combinations versus plate bound or soluble antibody (Table 2). We hypothesized that this enhanced stimulation is due to cellular aggregation on the SWNT-stimulus system. Preferential aggregation of T cells onto 3 M $HNO_3/LiBH_4$ SWNT during stimulation was confirmed qualitatively by comparing the cellular proliferation of fluorescently labeled T cells around anti-CD3 immobilized on SWNT versus blank

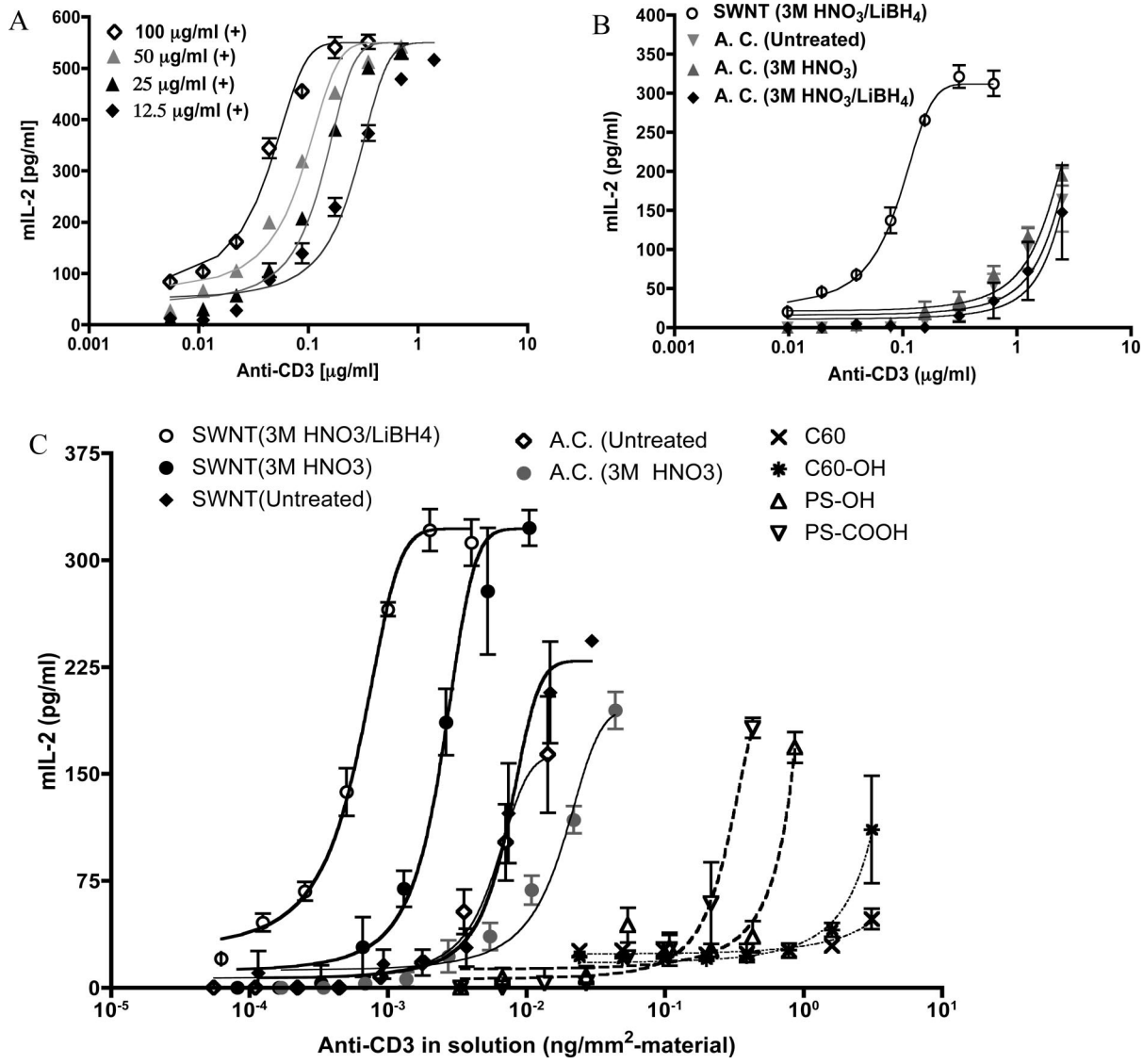

Figure 5. Impact of surface area on presenting antibodies for T cell stimulation. (A) Titration of anti-CD3 adsorbed SWNT and its effect on T cell stimulation. T cell stimulation was performed with a concentration of antibody-adsorbed SWNT at 100 μg/ml (+), 50 μg/ml (+), 25 μg/ml (+), and 12.5 μg/ml (+). All groups were treated with the same amount of anti-CD3 during adsorption. (B) Comparative T cell stimulation between 3 M HNO_3/$LiBH_4$ SWNT and a high surface area control material, activated carbon (A.C.). All materials were used at a concentration of 50 μg/ml, and initially loaded with the same concentration of anti-CD3. (C) Comparative T cell stimulation by multiple high surface area materials, normalized to the antibody per material surface area.

SWNT (Figure 4B). In these images, we observed selective aggregation of T cells around anti-CD3 adsorbed onto 3 M HNO_3/$LiBH_4$ SWNT scaffolds as seen in (T cells + SWNT + anti-CD3) when compared with 3 M HNO_3/$LiBH_4$ SWNT alone (T cells + SWNT).

To determine the effect of surface treatment on antibody adsorption and levels of T cell stimulation, we incubated anti-CD3 adsorbed onto treated and untreated SWNT bundles with T cells and measured T cell activation (Figure 4C). The response observed in 3 M HNO_3 /$LiBH_4$ SWNT was more pronounced than other SWNT groups. Modeling parameters from Table 2 show that half-maximal stimulation correlated with this observation. The log [EC50] value for 3 M HNO_3/$LiBH_4$ SWNT was the smallest (0.090) when compared with other groups (0.278 for 3 M HNO_3 and 0.973 for untreated). Chemical treatments alter surface functional groups as well as increase the surface area of SWNT bundles (Figure 2B). T cell activation by antibody adsorbed to functionalized 200 nm polystyrene nanoparticles (PS) indicates however that T cell stimulation is not affected by altering surface chemistry from carboxylate groups (mimicking 3 M HNO_3 treatment) or hydroxyl groups ($LiBH_4$ reduction after oxidation; see Supporting Information). Thus, the vast surface area of 3 M HNO_3/$LiBH_4$-treated SWNT bundles is primarily responsible for the observed increase in T cell stimulation. Additionally, these data demonstrate that chemical treatment can be used to tune the extent of protein adsorption and, in turn, to control the degree of T cell stimulation.

Levels of T cell stimulation can be modulated by varying the concentration of SWNT-stimulus bundles and keeping the amount of anti-CD3 constant during pretreatment (Figure 5A). T cells stimulated with SWNT bundles were responsive

to the density of SWNT in a concentration-dependent manner. Model fits from Table 2 show a correlation between the SWNT concentration and the half-maximal T cell response. This suggests that overall contact area facilitating a high density of antigen-presentation is a determinant factor for the observed efficiency of SWNT-stimuli on T cell stimulation.

To further investigate the effect of the SWNT surface area on T cell activation, we studied the stimulation potential of other high surface area materials after antibody adsorption. We first compared stimulation from activated carbon (1762 m^2/g) because of the similarity of this material to SWNT bundles. We additionally attempted to increase the surface area of the activated carbon as we did previously with SWNT bundles; but 3 M HNO_3 treatment resulted in a reduction[44] of the overall surface area (down to 573 m^2/g), and 3 M $HNO_3/LiBH_4$ treatment yielded a sample with an indeterminate surface area (see Table 3). As shown in Figure 5B, stimulation with all activated carbon samples is well below that of 3 M HNO_3/$LiBH_4$-treated SWNT bundles. However, the data in Figure 5B do not account for surface area differences. Thus, we normalized antibody presentation by surface area in Figure 5C. In this panel, we additionally show stimulation by 200 nm polystyrene beads (29 m^2/g), C60 and hydroxylated C60 (C60-OH; both estimated[45] at 4 m^2/g). Despite the high surface area of all materials, treated SWNT bundles on an antibody per area basis displayed the highest activation potential, as demonstrated by the Log [EC50] values (see Table 2), and in agreement with the protein adsorption superiority of this material (see Supporting Information Figure 2B). These data support the unique capability of SWNT bundles to enhance T cell stimulation.

The present study describes a new application for carbon nanotubes, as an effective surface for stimulation of cellular targets that rely on a high local density of stimulus for activation. A method was established for modulation of the surface area of SWNT by chemical treatment, which enhanced protein adsorption. High-density presentation of protein stimuli induces effective cellular activity. This correlation was studied within the context of T cell activation, a cell system that critically relies on and reads out a stimulus contact for physiological function. The large active surface area offered by SWNT is necessary for effective artificial antigen presentation, and we have exploited this property of SWNT to transform this material into a tunable platform for T cell stimulation. Even when antibody presentation is normalized by surface area, SWNT-antigen presenting bundles are more effective T cell stimulators than other materials, suggesting that they possess unique properties associated with the presentation of T cell antigens.

Previous studies with T cell stimulation highlight several facts that explain why SWNT bundles with adsorbed anti-CD3 functions as an excellent stimulation medium. First, clustering of T cell antigens impacts the T cell response by increasing the avidity of interaction to the antigen-presenting surface.[46–49] Second, immobilizing stimulating antibodies enhances their functional avidity for T cell activation.[46,48,50,51] Thus, superior stimulation of T cells can be observed with plate-bound anti-CD3 or anti-CD3 bound to an artificial antigen-presenting substrate compared with stimulation with free antibody in solution.[32,51] Third, increasing the negative charge of an antigen-presenting surface may further enhance its interactions with T cells because the surface charge becomes similar to professional antigen-presenting cells (cells adept at stimulating T cell responses such as mature dendritic cells), which combine high avidity interactions in an environment that displays negatively charged phospholipids heads and sugar groups.[48,52] Thus, a suggested mechanism for the enhanced stimulation response with treated SWNT surface may involve a combination of local clustering of the antibody stimuli in defect regions and the chemical nature of the environment surrounding these clusters. This high local concentrations of stimulus, in combination with the electronegativity of the acid-treated SWNT bundles, could explain why anti-CD3 at low overall concentrations when immobilized on the treated SWNT trigger such enhancement in T cell stimulation. Ultimately, this present application of SWNT bundles is ideal for ex vivo therapeutic stimulation of T cells, which requires efficient expansion of T cells outside the body with a robust stimulus. The potential offered by this application could be translated to other physiological systems requiring effective ligand presentation.

Acknowledgment. This work was supported by the Yale Institute of Nanoscience and Quantum Engineering (YINQE) and partially by an NSF Career Award (0747577) to T.M.F. We would like to acknowledge Dr. Victoria Ying, Michael Look, Michaela Panter, Codruta Zoican, Zhenting Jiang, and Andrea Brock for their assistance in this study.

Supporting Information Available: Materials and methods, physical characterization of treated and untreated A.C., adsorption isotherm of BSA and antibody, enhanced stimulation of T cells by anti-CD3 adsorbed onto SWNT, and model fit parameters to a concentration-response parametric model. This material is available free of charge via the Internet at http://pubs.acs.org.

References

(1) Ouyang, M.; Huang, J. L.; Lieber, C. M. *Acc. Chem. Res.* **2002**, *35*, 1018–1025.
(2) Feazell, R. P.; Nakayama-Ratchford, N.; Dai, H.; Lippard, S. J. *J. Am. Chem. Soc.* **2007**, *129*, 8438–8439.
(3) Kam, N. W. S.; Jessop, T. C.; Wender, P. A.; Dai, H. J. *J. Am. Chem. Soc.* **2004**, *126*, 6850–6851.
(4) Sitharaman, B.; Kissell, K. R.; Hartman, K. B.; Tran, L. A.; Baikalov, A.; Rusakova, I.; Sun, Y.; Khant, H. A.; Ludtke, S. J.; Chiu, W.; Laus, S.; Tóth, E.; Helm, L.; Merbach, A. E.; Wilson, L. J. *Chem. Commun.* **2005**, 3915–3917.
(5) Wang, Y.; Iqbal, Z. *J. Minerals* **2005**, *57*, 27–29.
(6) Bianco, A.; Kostarelos, K.; Prato, M. *Curr. Opin. Chem. Biol.* **2005**, *9*, 674–9.
(7) Pantarotto, D.; Partidos, C. D.; Graff, R.; Hoebeke, J.; Briand, J. P.; Prato, M.; Bianco, A. *J. Am. Chem. Soc.* **2003**, *125*, 6160–6164.
(8) Williams, K. A.; Veenhuizen, P. T. M.; de la Torre, B. G.; Eritja, R.; Dekker, C. *Nature* **2002**, *420*, 761–761.
(9) Pantarotto, D.; Briand, J. P.; Prato, M.; Bianco, A. *Chem. Commun.* **2004**, 16–17.
(10) Kam, N. W. S.; Liu, Z.; Dai, H. J. *J. Am. Chem. Soc.* **2005**, *127*, 12492–12493.

(11) Asuri, P.; Bale, S. S.; Pangule, R. C.; Shah, D. A.; Kane, R. S.; DordickJ. S. *Langmuir* **2007**, *23*, 12318–12321.
(12) Karajanagi, S. S.; Vertegel, A. A.; Kane, R. S.; Dordick, J. S. *Langmuir* **2004**, *20*, 11594–11599.
(13) Pardoll, D. M. *Nat. Rev. Immunology* **2002**, *2*, 227–38.
(14) June, C. H. *J. Clinical Investigation* **2007**, *117*, 1204–1212.
(15) Gattinoni, L.; Powell, D. J.; Rosenberg, S. A.; Restifo, N. P. *Nat. Rev. Immunology* **2006**, *6*, 383–393.
(16) Suvas, S.; Azkur, A. K.; Kim, B. S.; Kumaraguru, U.; Rouse, B. T. *J. Immunology* **2004**, *172*, 4123–4132.
(17) Dudley, M. E.; Rosenberg, S. A. *Nat. Rev. Cancer* **2003**, *3*, 666–675.
(18) Morgan, R. A.; Dudley, M. E.; Wunderlich, J. R.; Hughes, M. S.; Yang, J. C.; Sherry, R. M.; Royal, R. E.; Topalian, S. L.; Kammula, U. S.; Restifo, N. P.; Zheng, Z.; Nahvi, A.; de Vries, C. R.; Rogers-Freezer, L. J.; Mavroukakis, S. A.; Rosenberg, S. A. *Science* **2006**, *314*, 126–129.
(19) Zhou, J.; Dudley, M. E.; Rosenberg, S. A.; Robbins, P. F. *J. Immunotherapy* **2005**, *28*, 53–62.
(20) Dudley, M. E.; Wunderlich, J. R.; Shelton, T. E.; Even, J.; Rosenberg, S. A. *J. Immunotherapy* **2003**, *26*, 332–342.
(21) Prakken, B.; Wauben, M.; Genini, D.; Samodal, R.; Barnett, J.; Mendivil, A.; Leoni, L.; Albani, S. *Nat. Med.* **2000**, *6*, 1406–10.
(22) Oelke, M.; Maus, M. V.; Didiano, D.; June, C. H.; Mackensen, A.; Schneck, J. P. *Nat. Med.* **2003**, *9*, 619–24.
(23) Kim, J. V.; Latouche, J. B.; Riviere, I.; Sadelain, M. *Nat. Biotechnol.* **2004**, *22*, 403–410.
(24) Andersen, P. S.; Menne, C.; Mariuzza, R. A.; Geisler, C.; Karjalainen, K. *J. Biol. Chem.* **2001**, *276*, 49125–32.
(25) Gonzalez, P. A.; Carreno, L. J.; Coombs, D.; Mora, J. E.; Palmieri, E.; Goldstein, B.; Nathenson, S. G.; Kalergis, A. M. *Proc. Natl. Acad. Sci. U.S.A.* **2005**, *102*, 4824–9.
(26) Grakoui, A.; Bromley, S. K.; Sumen, C.; Davis, M. M.; Shaw, A. S.; Allen, P. M.; Dustin, M. L. *Science* **1999**, *285*, 221–7.
(27) Monks, C. R.; Freiberg, B. A.; Kupfer, H.; Sciaky, N.; Kupfer, A. *Nature* **1998**, *395*, 82–6.
(28) Anderson, A. O.; Shaw, S. *Immunity* **2005**, *22*, 3–5.
(29) Hu, H.; Zhao, B.; Itkis, M. E.; Haddon, R. C. *J. Phys. Chem. B* **2003**, *107*, 13838–13842.
(30) Liang, F.; Sadana, A. K.; Peera, A.; Chattopadhyay, J.; Gu, Z. N.; Hauge, R. H.; Billups, W. E. *Nano Lett.* **2004**, *4*, 1257–1260.
(31) Hemraj-Benny, T.; Bandosz, T. J.; Wong, S. S. *J. Colloid Interface Sci.* **2008**, *317*, 375–382.
(32) Kruisbeek, M. A.; Shevach, E.; Thornton, M. A. *Current Protocols in Immunology;* John Wiley & Sons, Inc.: New York, 2004.
(33) Johnson, E. W.; Jones, L. A.; Kozak, R. W. *J. Immunology* **1992**, *148,* 63–71.
(34) Papadimitrakopoulos, F. Bulk Separation of Semiconducting and Metallic Single Wall Nanotubes. 20040232073, 2004.
(35) Cinke, M.; Li, J.; Chen, B.; Cassell, A.; Delzeit, L.; Han, J.; Meyyappan, M. *Chem. Phys. Lett.* **2002**, *365*, 69–74.
(36) Park, T. J.; Banerjee, S.; Hemraj-Benny, T.; Wong, S. S. *J. Mater. Chem.* **2006**, *16*, 141–154.
(37) Thommes, M.; Smarsly, B.; Groenewolt, M.; Ravikovitch, P. I.; Neimark, A. V. *Langmuir* **2006**, *22*, 756–764.
(38) Valenti, L. E.; Fiorito, P. A.; Garcia, C. D.; Giacomelli, C. E. *J. Colloid Interface Sci.* **2007**, *307*, 349–356.
(39) Magrez, A.; Kasas, S.; Salicio, V.; Pasquier, N.; Seo, J. W.; Celio, M.; Catsicas, S.; Schwaller, B.; Forro, L. *Nano Lett.* **2006**, *6*, 1121–1125.
(40) Porter, A. E.; Gass, M.; Muller, K.; Skepper, J. N.; Midgley, P. A.; Welland, M. *Nature* **2007**, *2*, 713–717.
(41) Shvedova, A. A.; Castranova, V.; Kisin, E. R.; Schwegler-Berry, D.; Murray, A. R.; Gandelsman, V. Z.; Maynard, A.; Baron, P. *J. Toxicol. Environ. Health Part A* **2003**, *66*, 1909–26.
(42) Dumortier, H.; Lacotte, S.; Pastorin, G.; Marega, R.; Wu, W.; Bonifazi, D.; Briand, J. P.; Prato, M.; Muller, S.; Bianco, A. *Nano Lett.* **2006**, *6*, 1522–1528.
(43) Modeling fits of IL-2 release from T cells was performed using Prism Version 4.0b from Graphpad Software (2004). A sigmoidal response was used: $Y = \alpha+\beta\text{-}\alpha/1 + 10^{(Log(EC50)\text{-}X)}$ where X is the logarithm of concentration, Y is the response, α and β are the initial and final responses respectively.
(44) Niyogi, S.; Hamon, M. A.; Hu, H.; Zhao, B.; Bhowmik, P.; Sen, R.; Itkis, M. E.; Haddon, R. C. *Acc. Chem. Res.* **2002**, *35*, 1105–13.
(45) Vogel, W. *Appl. Phys. A-Mater. Sci. Process.* **1996**, *62*, 295–301.
(46) Grakoui, A.; Bromley, S. K.; Sumen, C.; Davis, M. M.; Shaw, A. S.; Allen, P. M.; Dustin, M. L. *Science* **1999**, *285*, 221–227.
(47) Dustin, M. *Immunity* **2004**, *21*, 305–314.
(48) Andersen, P. S.; Menné, C.; Mariuzza, R. A.; Geisler, C.; Karjalainen, K. *J. Biol. Chem.* **2001**, *276*, 49125–49132.
(49) Fahmy, T. M.; Bieler, J. G.; Edidin, M.; Schneck, J. P. *Immunity* **2001**, *14*, 135–143.
(50) Mossman, K. D.; Campi, G.; Groves, J. T.; Dustin, M. L. *Science* **2005**, *310*, 1191–1193.
(51) Steenblock, E. R.; Fahmy, T. M. *Molecular Therapy* **2008**, *16*, 765–772.
(52) Bell, G. I.; Dembo, M.; Bongrand, P. *Biophys. J.* **1984**, *45*, 1051–1064.

NL080332I